NIH Public Access
Author Manuscript
J Neurosci Res. Author manuscript; available in PMC 2013 March 22.

Published in final edited form as:
J Neurosci Res. 2010 February 1; 88(2): 290–303. doi:10.1002/jnr.22206.

IDENTIFICATION OF VESTIBULOOCULAR PROJECTION NEURONS IN THE DEVELOPING CHICKEN MEDIAL VESTIBULAR NUCLEUS

Adria Gottesman-Davis and **Kenna D. Peusner**
Department of Anatomy and Regenerative Biology, George Washington University Medical Center Washington, DC 20037

Abstract

Biocytin was injected into the oculomotor, trochlear, or abducens nucleus on one side using isolated chicken brainstem preparations or brain slices to identify the medial vestibular nucleus (MVN) neurons projecting to these targets. Oculomotor nucleus injections produced retrogradely labeled neurons in the contralateral ventrolateral MVN (MVN_{VL}), with few labeled neurons in the ipsilateral MVN_{VL}, and rarely in the dorsomedial MVN on either side. Labeled MVN_{VL} neurons were identified as stellate (95%) and elongate cells (5%). Trochlear nucleus injections produced a similar pattern of MVN neuron labeling. Abducens nucleus injections resulted in retrogradely labeled stellate (87%) and elongate (13%) neurons in the MVN_{VL} which had smaller cell bodies than those projecting to the oculomotor nucleus. Anteroposteriorly, labeled MVN_{VL} neurons were coextensive with the tangential nucleus, with neurons projecting to the oculomotor nucleus distributed lateral to and intermixed with the more medially situated neurons projecting to the abducens nucleus. The fundamental pattern of vestibuloocular projecting neurons was similar at both embryonic ages studied, E16 and E13. In contrast to mammals, where most vestibuloocular projection neurons reside within the MVN, the majority of retrogradely labeled neurons in these chicken preparations were found within the ventrolateral vestibular, descending vestibular, and tangential nuclei. The morphological identification and mapping of vestibuloocular projection neurons in the chicken MVN described here represents the first step in a systematic evaluation of the relationship between avian vestibuloocular neuron structure and function.

Keywords

extracellular biocytin dye; retrograde dye transport; vestibuloocular reflex neurons

INTRODUCTION

The medial vestibular nucleus (MVN) is the largest vestibular nucleus in humans (Alvarez et al., 1998), and is present throughout vertebrate phylogeny. Among the four main vestibular nuclei in vertebrates, the MVN is studied most extensively (for review, see Paterson et al., 2004). The MVN contains diverse neuron classes, including the second-order neurons participating in the three-neuron vestibulocollic, vestibulospinal, and vestibuloocular reflex (VOR) pathways (for review, see Straka et al., 2005). The relative simplicity of these reflexes makes them attractive for studying sensorimotor signal processing during

Correspondence to: Kenna D. Peusner, PhD Department of Anatomy and Regenerative Biology George Washington University Medical Center 2300 I Street NW, Washington, DC 20037 Phone: 202-994-3489; Fax: 202-994-8885; anakdp@gwumc.edu.

NIH-PA Author Manuscript
NIH-PA Author Manuscript
NIH-PA Author Manuscript

NIH-PA Author Manuscript

NIH-PA Author Manuscript

NIH-PA Author Manuscript

development, adaptation to changing stimuli, and recovery of function after lesions (e.g., Dieringer et al., 1984; Yamanaka et al., 2000).

From studies on other sensory systems, it is known that neurons with different inputs, outputs, and morphology serve different functions in signal processing (e.g., Feng et al., 1994; Ostapoff et al., 1994), and respond differentially to deafferentation (e.g., Francis and Manis, 2000). Three nuclei in the brainstem, the oculomotor, trochlear and abducens, which innervate the extrinsic eye muscles controlling eyeball movements, are known to receive input from MVN neurons. In most studies of the MVN, these VOR projection neurons are not distinguished from other neuron classes within the nucleus, which include those projecting to the contralateral vestibular nuclei, thalamus, cerebellum, and spinal cord, as well as interneurons (for review, see Highstein and Holstein, 2006). The analysis of the role of neuron class on signal processing is limited by the inability to target specific neuron classes for recordings in brain slice preparations.

The chicken is an advantageous experimental model due to its short gestation period, its in ovo accessibility to experimental manipulation, and its rich history in developmental biology. In addition, the chicken is precocious in its vestibular development, since hatchlings can stand and generate vestibular-mediated behaviors within hours of birth (Rogers, 1995; Shao et al., 2004, 2006a). Finally, compared to quadruped, the bipedal chicken may offer a more straightforward extrapolation to humans for investigating vestibular mechanisms, since the development of uprightness demands an improved sense of balance (Tobias, 1992).

So far, VOR connections have been traced extensively in the chicken and other vertebrates primarily by using extracellular injections of horseradish peroxidase (HRP) (e.g. Wold, 1978; McCrea et al., 1980; Labandeira-Garcia et al., 1989, 1991a, b; Cox and Peusner, 1990; Petursdottir, 1990; Arends et al., 1991). While HRP injections produce robust retrograde neuron labeling, fluorescent biocytin dye combined with confocal imaging provides higher resolution of cellular details from the retrogradely labeled neurons. In addition, HRP requires a 24 hour survival time, while biocytin retrograde labeling is achieved within hours after the injection. Moreover, fluorescently-conjugated biocytin used here provided better visualization of the morphology of the retrogradely labeled neurons. Biocytin was injected into the target nucleus contained within either a brain slice or brainstem placed in a culture dish, both of which permitted better visualization of the injection pipet and target nucleus for dye placement than can be achieved using whole animals. The in vitro preparations were particularly useful for labeling chick embryonic neurons, which are not readily accessible in ovo for dye injections requiring a delay for transport.

The present experiments represent the first step in the assembly of a classification scheme for VOR neurons in the chicken MVN, by determining the cell types and their axon pathways, and placing the neurons in a topographic map of the MVN.

METHODS

Experimental animals

Experiments were performed on white Leghorn chick embryos and hatchlings (*Gallus gallus*), purchased from CBT Farms (Chestertown, MD) as fertilized eggs and incubated in a laboratory egg incubator (GQF Manufacturing Company, model 1502), equipped with circulated air, temperature and humidity controls, and an egg rotation unit. The eggs were incubated until the appropriate embryonic age (13 and 16 days; E13, E16) and staged according to Hamburger and Hamilton (1951). Some eggs were allowed to hatch, with the hatchlings housed in cages equipped with heating lamps at the University's Animal Research

NIH-PA Author Manuscript

NIH-PA Author Manuscript

NIH-PA Author Manuscript

Facility until the selected age (H5). Animal protocols were approved by the Institutional Animal Care and Use Committee of the George Washington University. The experiments conformed to the International guidelines for the ethical treatment of animals, and care was taken to minimize the number of animals used and their suffering.

Brain dissection protocols

Brainstem preparations—After opening the eggshell, the embryos were removed and decapitated. Hatchlings were injected intramuscularly with ketamine (100 mg/kg) and xylazine (20 mg/kg; Phoenix Pharmaceutical, Inc), and decapitated after the withdrawal reflex was abolished. Under a dissecting microscope, the embryonic and hatchling brainstems were dissected free from the cranium, periodic capsule, and cerebellum in a solution of chilled (4°C), oxygenated artificial cerebrospinal fluid (ACSF). The brainstems were transferred immediately to a culture dish (ΔT; 2 ml; Bioptechs, Inc.) containing ACSF, which was maintained at room temperature (23-25°C) (Luksch et al., 1996). ACSF was superfused through the culture dish at a rate of 2-3 ml/min. The brainstem and pipet position were viewed under a dissecting microscope.

Brain slice preparations—Transverse sections (400 μm) of the embryonic brainstem were cut in cold ACSF (4°C) using a microslicer (Leica VT1000S) and razor blades (Feather blue blades; Ted Pella Inc.) (Shao et al., 2003, 2004, 2006a, b). Brain slices recovered for one hour in ACSF at room temperature in a Petri dish before transferring to a small, glass bottom recording chamber (180 μl, Warner Instruments). Brain slices were held in place in the chamber by a nylon net glued to a u-shaped flattened platinum wire. ACSF was perfused through the chamber (180 μl; Warner Instruments) at room temperature at a rate of 2-3 ml/min.

Solutions and injection pipets

ACSF contained (in mM): 126 NaCl, 3.5 KCl, 1.2 NaH_2PO_4, 1.3 $MgCl_2$, 2 $CaCl_2$, 26 $NaHCO_3$, and 10 D-glucose. ACSF was bubbled with 95% O_2/5%CO_2 to maintain the pH at 7.2-7.4. The osmolarity of ACSF was 310-320 mOsm. Pipets contained 2-4% biocytin dissolved in tris-buffered saline for injections into the brainstem preparations, while 4% biocytin was used to make injections in the brain slice preparations. Saline and tris-buffered saline solutions (Sigma) were found to be equally effective solvents for the pipet solution, and adding 2% dimethyl sulfoxide did not affect the results. Pipets were pulled from thin-walled (1.5 mm OD; 1.12 mm ID), borosilicate glass tube (World Precision Instruments) using a Brown/Flaming horizontal puller (P-87, Sutter Instruments). Pipets with tip diameters of 10 μm were used to make all the injections.

Biocytin extracellular injection protocols

Brainstem preparations—Pipets were advanced at an angle of 60° to the horizontal plane using a piezoelectric manipulator (Burleigh Inchworm 6000, Exfo Life Sciences Division). Biocytin solution was injected using a pneumatic pressure ejector (Picospritzer II, General Valve Corp), with an optimal setting of 20 puffs delivered at 5 PSI for 150-250 msec. After the injection, the brainstem preparations were kept in the culture dish for an additional 1.5 (E13), 2 (E16), or 3 hours (H5) to allow for the retrograde dye transport. Brainstems were viewed using a Nikon SMZ-10A dissecting microscope, with a final magnification of 2-3x. For the oculomotor (E13, n=4; E16, n=5; H5, n=1) and trochlear nuclei injections (E13, n=1; E16, n=5), the injection pipet was advanced through the dorsal surface of the brainstem to reach the target using surface features as landmarks. Methods for injecting biocytin into the abducens nucleus in the brainstem preparations (E13, n=3; E16, n=1) were similar to those described for the oculomotor nucleus injections, except that the

NIH-PA Author Manuscript

NIH-PA Author Manuscript

NIH-PA Author Manuscript

abducens nucleus was approached ventrally using the abducens nerve as a landmark. The ventral approach more readily avoided injecting label into the medial longitudinal fasciculus (MLF) and axons of vestibular nuclei neurons crossing the brainstem dorsal to the abducens nucleus. In all brainstem preparations, there was some biocytin labeling of ependymal cells lining the ventricular system (e.g., Fig. 3), most likely due to fast absorption of biocytin which leaked out of the pipet into the ventricle during dye injection.

Brain slice preparations—Transverse brain slices (400 μm thickness) were prepared for extracellular biocytin injection into the abducens nucleus at E13 (n=4 brain slices) and E16 (n=5 brain slices). Brain slices were taken from either the posterior part of the abducens nucleus, at the level of the anterior tangential nucleus and central MVN_{VL}, or the central part of the abducens nucleus, at the level of the MVN anterior to the crossed cochlear bundle, and positioned in the recording chamber with the posterior face up. Brain slices were viewed on a fixed-stage, upright microscope (Zeiss Axioskop FS-2), equipped with a 5x objective (NA, 0.12). Injection pipets were advanced at a 40° angle to the horizontal plane into the ipsilateral abducens nucleus using a piezoelectric manipulator (PCS-500, Burleigh Instruments, Exfo Life Sciences Division). The Axopatch-1D amplifier was used to inject the biocytin solution using 400 ms, 1.5 nA depolarizing current pulses at 1 Hz for 10 minutes. The stimulus was generated by a computer equipped with pClamp program (Clampex 9.2; Axon Instruments). After the injection, the brain slices remained in the chamber for 30-45 minutes.

Tissue processing

All preparations were fixed in 4% paraformaldehyde (PF) in 0.1 M phosphate buffer (PB, pH 7.4) overnight in the refrigerator. The next day, the brainstems were sectioned at 300 μm thickness using a vibratome (Oxford) into horizontal or transverse sections, which were then placed in 0.1 M PB (pH 7.4) and processed immediately for biocytin visualization. Brain slices were processed for biocytin detection without further sectioning. Biocytin was detected in tissue sections and brain slices using streptavidin Alexa Fluor 647 (Molecular Probes). Briefly, the tissue sections and brain slices were rinsed in 0.1 M phosphate buffered saline (PBS) containing 0.1% Triton X-100 (PBS-T), treated with 50% alcohol in PBS (20 minutes), and then rinsed with PBS-T (three times, 5 minutes each). Next, the sections and slices were incubated in streptavidin/Alexa Fluor 647 overnight, rinsed in PBS-T, and then mounted on glass slides, air dried, and coverslipped with antifading, water-soluble medium (Fluoromount G; Electron Microscopy Sciences).

Image acquisition

Conventional fluorescence microscopy—Biocytin-labeled neurons were observed on an Olympus BX60, equipped with a computer program (Image Pro Plus, Media Cybernetics) and 4x objective (NA 0.4), to determine the regions containing retrogradely-labeled neuron cell bodies.

Confocal microscopy—Labeled neurons in the tissue sections and brain slices were observed on an Olympus IX70 inverted microscope, equipped with BioRad confocal hardware (MRC 1024 ES, Bio-Rad Lab) and 10x UPlanFl (NA, 0.3), 20x PlanApo (NA, 0.70), and 40x Apo/340 (NA, 1.35) objectives. Excitation for Alexa Fluor 647 was achieved using a Kr/Ar laser, emitting at 647 nm. Confocal images at 10x were used to survey the regions containing retrogradely labeled neuron cell bodies, while 20x and 40x images were used to visualize the cell body size and shape, and dendritic morphology. A series of confocal images was collected with each image frame containing $(512)^2$ pixels. Each final confocal image was a function of the persistent pixels from four scans (Kalman x4 collection filter).

NIH-PA Author Manuscript

NIH-PA Author Manuscript

NIH-PA Author Manuscript

Image analysis

Only those preparations with the injected dye restricted to one side of the brain and confined to the boundaries of the target nucleus were included in the evaluation of MVN neuron number, location, and morphology. For inclusion, the targeted nucleus was labeled with biocytin over its full anteroposterior, dorsoventral, and mediolateral extent. Preparations containing extensive dye spread into the MLF were excluded from the study. Besides labeling vestibuloocular neurons, significant dye spread into the MLF at the level of the oculomotor or trochlear nucleus could produce labeling of vestibulothalamic neurons, which project their axons further anterior (e.g., Wild, 1988). At the level of the abducens nucleus, dye encroachment into the MLF could label ascending vestibulothalamic and vestibuloocular axons, as well as descending vestibulocollic axons (see Discussion). From a total of 40 injections into the oculomotor nucleus in brainstem preparations, 10 preparations (H5, n=1: E16, n=5; E13, n=4) met these criteria. A total of 18 trochlear nucleus injections were made in brainstem preparations (E16, n=9; E13, n=9), with one E16 and one E13 included in the analysis. A total of 69 abducens nucleus injections were made in brainstem preparations (E16, n=32; E13, n=37), with one at E16 and three at E13 included in the analysis. For injections into the abducens nucleus in brain slice preparations, a total of 19 chicken embryos were sacrificed (E16, n=8; E13, n=11), with the abducens nucleus receiving injections in 16 brain slices at E16 and 27 brain slices at E13. From the total number of injected brain slices, five at E16 and four at E13 met the conditions for restricted dye injection, so they were included in the description of cell classes, but not in the counts of labeled neurons after injecting the target nucleus (Table I). Counts of retrogradely labeled neuron cell bodies in the MVN, other vestibular nuclei, and other brainstem nuclei were made using the brainstem preparations, viewed in 10x confocal images using Adobe Photoshop (version 9.0). Measurements of the cell body size, shape, and orientation, counts of dendrites, and determination of the axon pathways were made on 20x and 40x confocal images from both brainstem and brain slice preparations. Measurements of the long axis of MVN neuron cell bodies were not significantly different from brainstem and brain slice preparations, so the data were combined. Gain and offset were adjusted to improve contrast. Labeled neurons were counted when the pixel brightness was clearly above background levels.

At the ages studied, some neuron-neuron dye coupling has been reported in the embryonic tangential nucleus, with the incidence increasing from two coupled neurons at E13 to four coupled neurons at E16, but interneuronal dye coupling becomes negligible one week after hatching (Shao et al., 2008). Thus, we cannot exclude the possibility that some biocytin labeling of vestibular nuclei neurons was due to dye coupling, since the low molecular weight biocytin (MW, 372.5) used here readily passes through gap junction channels (Bruzzone et al., 1996).

Nomenclature

The vestibular nuclei were classified using the terminology of Ramon y Cajal (1908), Sanders (1929), Peusner and Morest (1977a), Cox and Peusner (1990), and Popratiloff and Peusner (2007). Other brainstem nuclei and important anatomical landmarks were identified by reference to several avian brain atlases (pigeon, Karten and Hodos, 1967; hatchling chicken, Kuenzel and Masson, 1988; Puelles et al., 2007). The injected side of the brainstem is indicated by an “x” and placed on the left side in all low power, photomicrographs (Figs. 3-5).

Three-dimensional reconstruction of MVN labeled with MAP2

Three-dimensional reconstruction of the chicken MVN was generated from tissue sections at three ages, E13, E16, and H5. Anesthetized chickens (H5, n=3) and embryos (E13, n=3;

NIH-PA Author Manuscript

NIH-PA Author Manuscript

NIH-PA Author Manuscript

E16, n=3) were perfused through the cardiovascular system with 4% PF in 0.1 M PB, pH, 7.4. Serial 50 μm (E16, H5) or 100 μm (E13) transverse sections of the brainstem were prepared using a vibratome (Oxford), and labeled with the neuron marker, MAP2, as previously described (Popratiloff and Peusner, 2007). Tissue sections were rinsed in PBS-T, treated with 50% alcohol in PBS (20 minutes), rinsed with PBST (3 times, 5 minutes each), and then incubated in 10% normal goat serum (NGS; 30 minutes), followed by incubation in primary mouse IgG antibody specific for MAP2 (recognizes MAP2A and MAP2B; MAP 3418, clone AP20, Chemicon) at a concentration of 1:250 at room temperature (14 hours). The next day, the sections were rinsed in PBS-T, and then incubated in 2% NGS in PBS-T (10 minutes). After rinsing in PBS-T (3 times, 5 minutes each), the sections were incubated in PBS-T containing secondary goat anti-mouse IgG conjugated to Alexa Fluor 488 (1:200; Molecular Probes) for MAP2 neuron labeling. Finally, the sections were rinsed in PBS-T as described above and mounted. MAP2 labeling reveals neuron cells bodies and dendrites, but does not label fibers, so nuclear boundaries were defined by dendritic and somatic clusters.

M Serial tissue sections labeled with MAP2 were studied and photographed using conventional fluorescence imaging (Olympus BX60, 4x objective). Outlines of important structures were drawn in blue (MVN), red (tangential nucleus, abducens nucleus, nucleus magnocellularis) or green (brainstem surface, midline, and cranial nerves) (Adobe Photoshop CS2) overlaying the MAP2 images. These outlines were combined and assembled using Image Pro Plus 3D-Reconstructer program (version 5.1, National Institutes of Health), with a Z step which approximated the section thickness.

MAP2-labeled tissue sections were used to survey MVN neuron cell body sizes at ages when the cell body morphology was distinct (H5, E16; see Fig. 1B). Confocal image stacks (20x) were collected from every third section, representing 150 μm intervals of the MVN in series throughout its anteroposterior extent. Neurons were visualized using Image J (National Institutes of Health), and five neurons were selected randomly and measured from each section. Neurons were selected when their nucleus was present in the plane of section and the outlines of the cell body were apparent. The longest axis of the cell body and the axis perpendicular to this were measured. Both MAP2 and biocytin-labeled neuron cell bodies were identified as small, medium, or large neurons according to the length of the longest cell axis, with small neurons ranging from 11-19 μm, medium neurons 20-29 μm, and large neurons 30-47 um (Popratiloff and Peusner, 2007).

Statistical analysis

The values for cell body long and short axis were presented as the mean ± standard error of the mean. Differences in the measurements of the cell long axes were considered significant when $p<0.05$ (independent Student's t-test).

RESULTS

MVN topography

Situated in the anterior half of the medulla oblongata and posterior pons, the chicken MVN is elongated in its anteroposterior extent, curving in parallel with the fourth ventricle. Throughout most of its anteroposterior extent in transverse sections, the MVN appears subdivided by the crossed cochlear bundle into a distinctive dorsomedial part (MVN_{DM}), bordering the fourth ventricle, and a ventrolateral part (MVN_{VL}) (Fig. 1A). At levels anterior and posterior to the crossed cochlear bundle, the two parts of the MVN merge. In the present study, the MVN has been subdivided into five distinct levels along its anteroposterior extent (Fig. 2). (1) The posterior tip of the MVN is located at the same level as the posterior tip of nucleus magnocellularis. (2) The posterior tips of MVN_{VL} and

NIH-PA Author Manuscript

NIH-PA Author Manuscript

NIH-PA Author Manuscript

MVN_{DM} are located at about the same level as the posterior limit of the crossed cochlear bundle and posterior tip of the nucleus laminaris. (3) The mid-point of the MVN is found at different anteroposterior levels relative to the tangential nucleus, depending on age. (4) The anterior level at which MVN_{VL} and MVN_{DM} merge is located at about the same level as the anterior tip of the nucleus magnocellularis. (5) The anterior tip of the MVN is situated at about the same level as the anterior tips of the nucleus laminaris and abducens nucleus.

Although there are slight developmental shifts in the relative positions of important nuclear landmarks, the major features delineating the position of the MVN in the brainstem are consistent at the two embryonic ages studied. To determine whether these features are retained after hatching, the MVN was mapped at H5. At H5, the MVN measures about 1800 μm in its anteroposterior extent (Fig. 2A), while at E16 and E13, the MVN measures 1500 μm and 1200 μm, respectively (Figs. 2B, 2C). At H5, the MVN mid-point is located at the level of the posterior tangential nucleus, whereas at E16 and E13, the mid-point gradually shifts to the level of the central tangential nucleus. A survey of MVN neuron morphology was performed using the MAP2-labeled tissue sections prepared for the three-dimensional MVN maps at H5 and E16. All MAP2-labeled neurons appeared to be relatively round and multipolar (Figs. 1B, C). No significant differences were detected in the average cell body size for randomly selected neurons from MVN_{DM} and $MVN_{VL,}$ or from H5 and E16 preparations (23×16 μm, on average; n=55 neurons at H5; n=50 at E16).

Oculomotor nucleus injections

At all the ages investigated, the oculomotor nucleus was situated close to the midline of the brainstem. The subnuclei of the oculomotor nucleus are distinct in the E13 chicken, although the ventromedial subnuclei are fused partially at this age (Niimi et al., 1958). Despite increased distance between the ventromedial subnuclei by E16, robust connections persisted between the subnuclei at this and older ages, as found in the cat (Graf and Ezure, 1986). These connections could account for the dye transport to the contralateral nucleus seen in the present preparations (Fig. 3A).

Labeled fibers were found within the MLF, and traveled near the trochlear nucleus ipsilateral to the injection site (Fig. 3A). At the level of the abducens and vestibular nuclei, many labeled axons crossed the midline and then coursed contralateral to the injection site, while some axons remained on the ipsilateral side. Most ipsilateral and contralateral fibers ran laterally and then ascended, so that most of the cells bodies of origin of the labeled axons were located dorsal to the point where the axons crossed the midline (Fig. 4). In addition, some axons remained within the ipsilateral MLF and continued to descend to levels posterior to the vestibular nerve.

On the side contralateral to the injected oculomotor nucleus, labeled neurons were dispersed within a mediolaterally-directed band, which extended from the MVN to the lateral surface of the medulla oblongata, including neurons in the $MVN_{VL,}$ ventrolateral, descending, and tangential vestibular nuclei (Fig. 4B, C; Table I). In contrast, on the ipsilateral side, small, round clusters of labeled neurons were concentrated in the ventrolateral or descending vestibular nucleus. Retrogradely labeled MVN neurons were found primarily between levels 3 and 4 (Figs. 2 and 4B, C; Table II). In some experiments, a few scattered MVN neurons were detected anterior to level 4, predominantly on the contralateral side (not shown). In addition, a few retrogradely labeled MVN neurons were found between levels 2 and 3, but none were observed posterior to level 2 (Fig. 4D). This pattern was consistent at E16 and E13, and confirmed at H5 (n=1).

Most retrogradely labeled MVN neurons were found in the contralateral MVN_{VL} and, rarely, in the contralateral MVN_{DM}. A smaller number of labeled neurons were found in the

NIH-PA Author Manuscript

NIH-PA Author Manuscript

NIH-PA Author Manuscript

ipsilateral MVN_{VL}. No labeled neurons were detected in the ipsilateral MVN_{DM}. Retrogradely labeled MVN neurons were found predominantly at anteroposterior levels coextensive with the tangential nucleus. Labeled MVN_{VL} neurons were found across the full mediolateral extent of the nucleus on the side contralateral to injection, but on the ipsilateral side they were primarily located near the lateral border of MVN_{VL} with the ventrolateral vestibular nucleus (see Fig. 9).

After injecting the oculomotor nucleus, retrogradely labeled neuron cell bodies were also observed in the ventrolateral and descending vestibular nuclei, bilaterally (Fig. 4C, D; Table I). These neurons were stellate cells with medium-size cell bodies (26±0.8 μm, n=24 neurons; E16, n=1 animal; E13, n=1 animal) and 5-6 primary dendrites. These neurons were similar to the neurons of the descending vestibular nucleus injected intracellularly with biocytin in E13 chickens (Peusner and Giaume 1997). Routinely, retrogradely labeled neuron cell bodies were found in the tangential nucleus, bilaterally, with the contralateral side showing stronger labeling (Fig. 4C). The labeled neurons in the tangential nucleus were principal cells, based on cell body size (34±0.6 in their longest dimension; n=30 neurons; E16, n=1 animal; E13, n=1 animal) and their oval somatic shape (Peusner and Morest, 1977b). Retrogradely labeled neurons were seen routinely in the ipsilateral superior vestibular nucleus (Fig. 4B; Table I), and occasionally in the contralateral superior vestibular nucleus (Table I). These neurons had medium-size, multipolar cell bodies, with primary dendrites that were often hard to trace in these preparations.

Oculomotor nucleus injections typically produced strong retrograde labeling of neuron cell bodies in the contralateral abducens nucleus. The labeled neurons were mostly multipolar, with cell bodies ranging from 25-30 μm in their longest diameter (n=30 neurons; E16, n=3 animals; E13, n=3 animals). The labeled neurons were distributed throughout the mediolateral and dorsoventral extent of the nucleus, as described for abducens internuclear neurons in the adult chicken after HRP injections into the oculomotor nucleus (Fig. 2; Labandeira-Garcia et al., 1987). Finally, labeling of trochlear nucleus neurons was observed routinely following oculomotor nucleus injection (e.g., Fig. 3), which could be attributed to dye uptake by the dendrites of trochlear nucleus neurons which extend into the oculomotor nucleus (e.g., Evinger et al., 1987; Bacskai et al., 2008).

Trochlear nucleus injections

The trochlear nucleus is located immediately posterior to the oculomotor nucleus and adjacent to the fourth ventricle. Despite producing discrete unilateral injections into the trochlear nucleus, extensive neuron labeling was found invariably in the oculomotor nucleus. Based on finding labeled fibers passing through the trochlear nucleus after discretely injecting the oculomotor nucleus, the labeling of oculomotor nucleus neurons after trochlear injections was likely due to fibers coursing between the two nuclei. Accordingly, the present methods cannot be used to distinguish axons of vestibular nuclei neurons terminating in the trochlear nucleus from those terminating in the oculomotor nucleus. Moreover, since smaller dye injections were required for the smaller trochlear nucleus, fiber labeling was less intense and labeled axons were more difficult to trace.

In brainstem preparations, retrogradely labeled MVN neurons were found only on the contralateral side, with the majority in the MVN_{VL} (Fig. 5). A few retrogradely labeled neurons were also found in the contralateral MVN anterior to the anterior limit of the crossed-cochlear bundle (between levels 4 and 5), within the merged anterior portion of the MVN. Labeled neurons were found bilaterally in the ventrolateral vestibular nucleus, with stronger labeling on the contralateral side. Labeled neurons were found only in the contralateral descending vestibular nucleus. Neurons in the tangential nucleus were labeled on the contralateral side only at E13 (n=1), but labeling was bilateral at E16 (n=1). Like the

NIH-PA Author Manuscript

NIH-PA Author Manuscript

NIH-PA Author Manuscript

oculomotor nucleus injections, the labeled neurons which were visible in the tangential nucleus were principal cells, based on their cell body size and shape, and the medial course of their axons. A few retrogradely labeled neurons were found in the ipsilateral superior vestibular nucleus, and none in the contralateral nucleus.

Abducens nucleus injections

The abducens nucleus is situated ventral to the MVN, so both nuclei are present in transverse brainstem sections containing the posterior abducens nucleus (Fig. 6). Due to the proximity of these two nuclei, both brain slice and whole brainstem preparations were tested for ease of obtaining discrete biocytin injections into the abducens nucleus.

In whole brainstem preparations (E16, n=1; E13, n=3), a relatively small number of labeled neurons were found in the MVN after discrete abducens nucleus injections (Table I). As found with oculomotor and trochlear nuclei injections, the retrogradely labeled MVN neurons were found primarily between levels 3 and 4, with no labeled MVN neurons found posterior to level 2. Retrogradely labeled neurons were found in both the ipsilateral and contralateral MVN, primarily in the MVN_{VL}, with somewhat more neurons in the ipsilateral nucleus (see Fig. 9). After injecting the abducens nucleus in whole brainstem preparations, the majority of retrogradely labeled vestibular nuclei neurons were located bilaterally in the ventrolateral, descending, superior, and tangential vestibular nuclei (Table I). In the ventrolateral vestibular nucleus, the labeled neurons were mediumsize, multipolar neurons, while in the tangential nucleus, only the principal cells were labeled. Retrogradely labeled neurons were found also in the contralateral abducens nucleus, which were similar morphologically to those found in the injected abducens nucleus. Generally, labeled abducens nucleus neurons were neurons with medium-size (20-30 μm) and small cell bodies (10-15 μm) (n=35 neurons; E16, n=1 animal; E13, n=2 animals). The larger neurons most likely represented a mixture of abducens motor and large internuclear neurons, while the smaller neurons were likely abducens internuclear neurons (see Labandeira-Garcia et al., 1987).

Brain slice preparations contained a larger number of retrogradely labeled MVN_{VL} neurons at levels 3-3.9 (E16, n=2 animals; E13, n=1) and levels 4-5 (E16, n=3; E13, n=3) than after injecting the abducens nucleus in the whole brainstem preparations. It is possible that biocytin leakage from the injection site increased the amount of non-specific neuron labeling. In addition, the brain slices were limited to the anterior half of the MVN where the abducens nucleus is present (Fig. 2), so that labeled axons which continued beyond the limits of the brain slice were cut off before reaching their cell bodies. Accordingly, the findings from the brain slices preparations were excluded from counts of the number of labeled neurons (Tables I, II).

Cellular morphology of VOR projection neurons in the MVN

Labeled MVN_{VL} neurons, which projected to the oculomotor and trochlear nucleus, were predominantly stellate cells (95%) with medium-size cell bodies measuring 25×19 μm, on average, at E16 (n=92 neurons from 5 animals) (Fig. 7A) and 20×15 μm, on average, at E13 (n=72 neurons from 4 animals), with 3-6 primary dendrites. A second neuron population was classified as elongate cells (5%). The elongate cells had the long axis of their cell bodies at least twice as long as their short axis, measuring 30×14 μm, on average, at E16 (n=4 neurons from 3 animals) (Fig. 7B) and 27×12 μm, on average, at E13 (n=4 neurons from 2 animals). Elongate cells had fewer primary dendrites (2-5), on average, than the stellate cells. Stellate and elongate cells were dispersed throughout the MVN_{VL} dorsoventrally and mediolateral, while the stellate cells were found at levels 2-5 anteroposteriorly, with elongate cells concentrated at levels 3-5 (Table II).

NIH-PA Author Manuscript

NIH-PA Author Manuscript

NIH-PA Author Manuscript

There was no difference in the morphology of abducens projection neurons labeled in brain slices compared to those in brainstem preparations (Fig. 8). In both brainstem and brain slice preparations, the dendrites of the stellate and elongate cells projecting to the abducens nucleus were often weakly labeled compared to those of neurons projecting to the oculomotor and trochlear nuclei. Labeled MVN_{VL} neurons projecting to the abducens nucleus were found between anteroposterior levels 2-4 (Fig. 2, Table II). While the average cell body size for the abducens nucleus projection neurons was larger at E16 than at E13 ($p<0.001$), the fundamental morphology and number of dendrites of the stellate and elongate cells remained the same.

From neuron counts made on whole brainstem preparations after injecting the abducens nucleus, the labeled neurons projecting to the abducens nucleus were primarily stellate cells (87%) (Fig. 7C), with similar morphology to the stellate cells labeled after oculomotor nucleus injections (Figs. 7, 8). However, the stellate cells projecting to the abducens nucleus had fewer primary dendrites (2-5) and smaller cell bodies, measuring 22×16 μm, on average, at E16 (n=91 neurons from 1 brainstem and 5 brain slice preparations) and 18×12 μm, on average, at E13 (n=68 neurons from 3 brainstem and 4 brain slice preparations). In addition, a few elongate cells (13%) (Fig. 7D) were labeled, which were similar to, but smaller than the elongate cells projecting to the oculomotor nucleus, measuring 26×12 μm, on average, at E16 (n=13 neurons from 1 brainstem and 4 brain slice preparations) and 23×11 μm, on average, at E13 (n=12 neurons from 2 brainstem and 2 brain slice preparations). Overall, at both E16 and E13, MVN_{VL} neurons projecting to the oculomotor nucleus were significantly larger than those projecting to the abducens nucleus, regardless of laterality ($p<0.05$) (Fig. 10).

DISCUSSION

MVN neurons which participate in the VOR pathways are confined to the central two-thirds of the MVN_{VL} in the anteroposterior axis. These neurons are primarily stellate cells, with a few elongate cells interspersed. This work supports the hypothesis that neurons of the chicken MVN_{DM} have little or no involvement in the VOR pathways. In mammals, MVN_{DM} neurons project to the trigeminal motor nucleus (e.g., Shaw and Baker, 1983; Hinrichsen and Watson 1983; Cuccurazu et al., 2007) or cerebellum (Saxon and Beitz, 2000).

VOR connections in the chicken

In the present study, biocytin injections into the oculomotor, trochlear or abducens nucleus produced labeled VOR projection neurons which were highly diversified in their nucleus of origin, with bilateral projections from neurons in the medial, ventrolateral, descending, and tangential vestibular nuclei. A striking feature of our preparations was the mediolaterally extended band of retrogradely labeled neurons on the side contralateral to the injection site. This band cut across nuclear boundaries to include tangential, ventrolateral vestibular, and MVN neurons, and may reflect the rhombomeric origin of these neurons (Diaz and Glover, 2002). The general pattern of chick VOR projection pathways described here is consistent with past studies. Unilateral extracellular injections of horseradish peroxidase (HRP) into the oculomotor and/or trochlear nucleus of the adult chicken produced retrograde labeling of neuron cell bodies in a continuous band within the contralateral medial, descending, and tangential vestibular nuclei (Wold, 1978; Labandeira-Garcia et al., 1989). On the ipsilateral side, smaller, round clusters of neurons were labeled, concentrated in the ventrolateral, descending, tangential, and superior vestibular nuclei. This same pattern of neuron labeling was detected after dextran amine was placed in the MLF of E11 chicken embryos (Petursdottir, 1990). In all of these studies, non-vestibular neurons are labeled, with the most conspicuous labeling occurring in the abducens nucleus. Finally, we confirmed that a major

NIH-PA Author Manuscript

NIH-PA Author Manuscript

NIH-PA Author Manuscript

output of the tangential principal cells projected to the contralateral abducens nucleus (Cox and Peusner, 1990).

While the pattern of labeling produced by our injections is strikingly similar to the pattern observed in previous studies (e.g. Wold, 1978; Labandeira-Garcia et al., 1989), the number of MVN neurons projecting to the oculomotor and trochlear nuclei obtained here were considerably fewer. This may be attributed in part to the previous studies placing the MVN boundary more lateral into what is defined here and elsewhere as the ventrolateral vestibular nucleus (Ramon y Cajal, 1908; Karten and Hodos, 1967; Kuenzel and Masson, 1988; Puelles et al., 2007; Peusner and Morest, 1977a; Cox and Peusner, 1990; Popratiloff and Peusner, 2007). Indeed, our findings indicate that the MVN in the chicken is not the major source of VOR projection neurons.

Development of VOR circuitry in the chicken

In fluorescent dye tracer studies, axons from abducens motor neurons first contact the lateral rectus muscle around E3 (Wahl et al., 1994), whereas axons of oculomotor and trochlear nuclei neurons reach their muscle targets around E5-6 (Glover, 2003). Vestibuloocular axons invade the abducens nucleus around E3 and the oculomotor and trochlear nuclei around E5, but there is a delay of 1-2 days before the ingrown axons sprout collaterals within the target nuclei (Glover, 2003). Finally, primary vestibular fibers grow into the brainstem around E3 (Knowlton, 1967; Petralia and Peusner, 1991), but do not form synapses on second-order neurons of the tangential nucleus until E7.5 (Petralia and Peusner, 1990). Recordings of spontaneous synaptic activity from second-order vestibular neurons of the tangential nucleus indicate that both excitatory and inhibitory activity is present at low frequencies by E10 and continues to increase in older embryos and hatchlings (Shao et al., 2004; 2006b). Thus, the fundamental VOR circuitry has been laid down before the E13-E16 stages studied here, although neuronal growth and elaboration of synaptic connections will continue.

Comparison of mammalian and chicken VOR connections

The distribution of VOR projection neurons within the vestibular nuclei in mammals is similar to the pattern described in our chicken preparations, with some notable differences. HRP injections into the oculomotor nucleus of the rabbit revealed a band of labeled neurons on the side contralateral to the injection site (e.g, Labandeira-Garcia, 1991a, b), but in the rabbit this band is concentrated medially within the brainstem. This may reflect the absence of the tangential nucleus in mammals, which in the chicken represents a major source of VOR projection neurons. Additionally, in rabbits the lateral part of the band is found mainly posterior to the vestibular nerve root and abducens nucleus, whereas in the chicken, the band appeared coextensive with the primary vestibular fibers. In young postnatal mouse, unilateral injections of rhodamine dextran into the oculomotor nucleus produce strong retrograde labeling of neurons contralateral to the injection site, primarily confined to the MVN_{VL} (Sekirnjak and du Lac, 2006). On the ipsilateral side, labeled neurons were concentrated in the superior vestibular nucleus, with a few neurons in the ventrolateral vestibular nucleus. Thus, in the chicken, there is lateral displacement of VOR projection neurons and a shift toward more anterior levels of the brainstem compared to mammals. The pattern of VOR neuron distribution in the chicken could be related to their distinct head-bobbing gait, which is under the control of the visual system (Frost, 1978), and found only in those avians with laterally displaced eyes (Whiteside, 1967).

Our results confirmed the finding from HRP injections into the cat abducens nucleus, which revealed labeling of medium-size, multipolar neurons in the ipsi- and contralateral MVN_{VL} (McCrea et al., 1980). In addition, after wheat-germ agglutinin (WGA)-HRP injections were

NIH-PA Author Manuscript

NIH-PA Author Manuscript

NIH-PA Author Manuscript

made into the abducens nucleus of the squirrel monkey, MVN neurons projecting to the abducens nucleus were found mainly in the rostral MVN_{VL} (Belknap and McCrea, 1988).

Chicken and mammalian vestibuloocular collic reflex connections

In the present preparations, some axons were observed in the MLF posterior to the level of the vestibular nerve, suggesting that some labeled neurons could have axons which descend to the lower brainstem and/or spinal cord. Some tangential principal cells, with axons projecting to the contralateral abducens nucleus, send collateral branches in the MLF to high cervical levels of spinal cord, the vestibuloocular collic neurons (VOC; Cox and Peusner, 1990). VOC neurons likely coordinate head and eye movements. In mammals, VOC neurons are located in the lateral, medial and descending vestibular nuclei, and project to the abducens, oculomotor, and trochlear nuclei (e.g., Boyle et al., 1992). In the cat and monkey, about 25-75% of all VOR neurons whose axons run within the ascending MLF have axons coursing to the cervical spinal cord as VOC neurons (Isu et al., 1988; Minor et al., 1990). Possibly, some of the labeled neurons in our preparations were VOC neurons, but the termination of their descending axons was not traced.

Cellular morphology of VOR projection neurons in the MVN

In the present study, the anteroposterior location of VOR projection neurons in the MVN was mapped, their mediolateral distribution was established, and their characteristic morphologies were described. Previous studies have established that chick second-order vestibular neurons acquire many of their definitive morphological features by E13, such as cell body size and shape, and number of primary dendrites and dendritic branching pattern, and retain them after hatching (Peusner and Giaume, 1997). Both stellate and elongate cells were found after oculomotor, trochlear or abducens nucleus injections. Why these two cells types, with a clear predominance of stellate cells, are representative of VOR projection neurons in the MVN remains to be determined. The oculomotor-projecting stellate and elongate cells described here have strikingly similar morphologies to the VOR projection neurons in the mouse MVN (see Fig. 2, Sekirnjak and du Lac, 2006), and MVN neurons in the transgenic mouse, identified by their neurotransmitter content (see Fig. 1, Bagnall et al, 2007). Both stellate and elongate cells are described in the cochlear nuclei (e.g., Ostapoff et al., 1994) and ascending auditory brainstem nuclei (e.g., Zhao and Wu, 2001) where these morphologies correlate with distinct membrane properties and/or discharge patterns. The morphological classes detected in the central auditory system strengthen the case for a relationship between VOR neuron morphology and function. The MVN has no laminar arrangement to assist in sorting out distinct neuron classes. However, concern should be raised when data are averaged from diverse MVN neuron classes, since this could obscure key functional differences in neuron classes. Thus, the identification and localization of VOR projection neurons in the MVN represents a crucial first step in defining their roles in central vestibular signal processing.

Acknowledgments

The Authors gratefully acknowledge Drs. M. Shao and A. Popratiloff for helpful suggestions throughout the course of the work, Dr. J Hirsch for reading the manuscript, and Mr. X. Cai for excellent technical assistance.

This work was supported by NIH grant R01 DC00970 and NIH predoctoral fellowship grant 1 F31 DC008715.

LITERATURE CITED

Alvarez JC, Diaz C, Suarez C, Fernandez JA, Del Rey CG, Navarro A, Tolivia J. Neuronal loss in human medial vestibular nucleus. Anat Rec. 1998; 251:431–8. [PubMed: 9713981]

NIH-PA Author Manuscript

NIH-PA Author Manuscript

NIH-PA Author Manuscript

Arends JJA, Allan RW, Zeigler HP. Organization of the cerebellum in the pigeon (*Columba livia*): III. Corticovestibular connections with eye and neck premotor areas. J Comp Neurol. 1991; 306:273–289. [PubMed: 1711055]

Bacskai T, Veress G, Halasi G, Deak A, Racz E, Szekely G, Matesz C. Dendrodendritic and dendrosomatic contacts between oculomotor and trochlear motoneurons of the frog, Rana esculenta. Brain Res Bull. 2008; 75:419–423. [PubMed: 18331909]

Bagnall MW, Stevens RJ, du Lac S. Transgenic mouse lines subdivide medial vestibular nucleus neurons into discrete, neurochemically distinct populations. J Neurosci. 2007; 27:2318–2330. [PubMed: 17329429]

Belknap DB, McCrea RA. Anatomical connections of the prepositus and abducens nuclei in the squirrel monkey. J Comp Neurol. 1988; 268:13–28. [PubMed: 3346381]

Boyle R, Goldberg JM, Highstein SM. Inputs from regularly and irregularly discharging vestibular nerve afferents to secondary neurons in squirrel monkey vestibular nuclei. III. Correlation with vestibulospinal and vestibuloocular output pathways. J Neurophysiol. 1992; 68:471–484. [PubMed: 1527570]

Bruzzone R, White TW, Paul DL. Connections with connexins: the molecular basis of direct intercellular signaling. Eur J Biochem. 1996; 238:1–27. [PubMed: 8665925]

Cox RG, Peusner KD. Horseradish peroxidase labeling of the efferent and afferent pathways of the avian tangential vestibular nucleus. J Comp Neurol. 1990; 296:324–341. [PubMed: 2358540]

Cuccurazzu B, Deriu F, Tolu E, Yates BJ, Billig I. A monosynaptic pathway links the vestibular nuclei and masseter muscle motoneurons in rats. Exp Brain Res. 2007; 176:665–671. [PubMed: 17216144]

Diaz C, Glover JC. Comparative aspects of the hodological organization of the vestibular nuclear complex and related neuron populations. Brain Res Bull. 2002; 57:307–312. [PubMed: 11922978]

Dieringer N, Kunzle H, Precht W. Increased projection of ascending dorsal root fibers to vestibular nuclei after hemilabyrinthectomy in the frog. Exp Brain Res. 1984; 55:574–578. [PubMed: 6332031]

Evinger, C.; Graf, WM.; Baker, R. Extra-and intracellular HRP analysis of the organization of extraocular motoneurons and internuclear neurons in the guinea pig and rabbit. 1987.

Feng JJ, Kuwada S, Ostapoff EM, Batra R, Morest DK. A physiological and structural study of neuron types in the cochlear nucleus. I. Intracellular responses to acoustic stimulation and current injection. J Comp Neurol. 1994; 346:1–18. [PubMed: 7962705]

Francis HW, Manis PB. Effects of deafferentation on the electrophysiology of ventral cochlear nucleus neurons. Hearing Res. 2000; 149:91–105.

Frost BJ. The optokinetic basis of head-bobbing in the pigeon. J Exp Biol. 1978; 74:187–195.

Glover JC. The development of vestibulo-ocular circuitry in the chicken embryo. J Physiol. 2003; 97:17–23.

Graf W, Ezure K. Morphology of vertical canal related second order vestibular neurons in the cat. Exp Brain Res. 1986; 63:35–48. [PubMed: 3732448]

Hamburger V, Hamilton H. A series of normal stages in the development of chick embryo. J Morphol. 1951; 88:49–92.

Highstein SM, Holstein GR. The anatomy of the vestibular nuclei. Prog Brain Res. 2005; 151:157–203. [PubMed: 16221589]

Hinrichsen CFL, Watson CD. Brain stem projections to the facial nucleus of the rat. Brain Behav Evol. 1983; 22:153–163. [PubMed: 6303494]

Isu N, Uchino Y, Nakashima H, Satoh S, Ichikawa T, Watanabe S. Axonal trajectories of posterior canal-activated secondary vestibular neurons and their coactivation of extraocular and neck flexor motoneurons in the cat. Exp Brain Res. 1988; 70:181–191. [PubMed: 3402563]

Karten, HJ.; Hodos, W. A Stereotaxic Atlas of the Brain of the Pigeon (*Columba Livia*).. The Johns Hopkins Press; Baltimore, MD: 1967.

Knowlton VY. Effects of extraembryonic membrane deficiency on differentiation of the embryonic avian brain and sense organs. Acta Anat. 1967; 66:420–45. [PubMed: 6058705]

Kuenzel, WJ.; Masson, M. A Stereotaxic Atlas of the Brain of the Chick (*Gallus Domesticus*).. The Johns Hopkins Press; Baltimore, MD: 1988.

NIH-PA Author Manuscript

NIH-PA Author Manuscript

NIH-PA Author Manuscript

Labandeira-Garcia JL, Guerra-Seijas MJ, Segade LAG, Suarez-Nuñez JM. Identification of abducens motoneurons, accessory abducens motoneurons, and abducens internuclear neurons in the chick by retrograde transport of horseradish peroxidase. J Comp Neurol. 1987; 259:140–149. [PubMed: 3584553]

Labandeira-Garcia JL, Guerra-Seijas MJ, Labandeira-Garcia JA, Jorge-Barreiro FJ. Afferent connections of the oculomotor nucleus in the chick. J Comp Neurol. 1989; 282:523–534. [PubMed: 2723150]

Labandeira-Garcia JL, Guerra-Seijas MJ, Labandeira-Garcia JA, Jorge-Barreiro FJ. Distribution of the vestibular neurons projecting to the oculomotor and trochlear nuclei in rabbits. Brain Behav Evol. 1991a; 37:111–124. [PubMed: 2054584]

Labandeira-Garcia JL, Guerra-Seijas MJ, Castroviejo-Bolivar MA, Jorge-Barreiro FJ. A comparative study of the tangential-oculomotor projection. J fur Hirnforschung. 1991b; 32:203–209.

Luksch H, Walkowiak W, Monoz A, ten Donkelaar HJ. The use of in vitro preparations of the isolated amphibian central nervous system in neuroanatomy and electrophysiology. J Neurosci Meth. 1996; 70:91–102.

McCrea RA, Yoshida K, Berthoz A, Baker R. Eye movement related activity and morphology of second order vestibular neurons terminating in the cat abducens nucleus. Exp Brain Res. 1980; 40:468–473. [PubMed: 7439286]

Minor LB, McCrea RA, Goldberg JM. Dual projections of secondary vestibular axons in the medial longitudinal fasciculus to extraocular motor nuclei and the spinal cord of the squirrel monkey. Exp Brain Res. 1990; 83:9–21. [PubMed: 2073953]

Niimi K, Sakai T, Takasu J. The ontogenetic development of the oculomotor nucleus in the chick. Tokushima J Exp Med. 1958; 5:311–325.

Ostapoff EM, Feng JJ, Morest DK. A physiological and structural study of neuron types in the cochlear nucleus. II. Neuron types and their structural correlation with response properties. J Comp Neurol. 1994; 346:19–42. [PubMed: 7962710]

Paterson JM, Menzies JRW, Bergquist F, Dutia MB. Cellular mechanism of vestibular compensation. Neuroembryol Aging. 2004; 3:183–193.

Pétursdóttir G. Vestibulo-ocular projections in the 11-day chicken embryo: pathway specificity. J Comp Neurol. 1990; 297:283–297. [PubMed: 2164534]

Petralia RS, Peusner KD. Ultrastructural study of synapses at time of neuronal migration and early differentiation in the tangential vestibular nucleus of the chick embryo in vivo. J Comp Neurol. 1990; 292:231–245. [PubMed: 2319011]

Petralia RS, Peusner KD. The earliest ultrastructural development of the tangential vestibular nucleus in the chick embryo. J Comp Neurol. 1991; 310:82–93. [PubMed: 1719038]

Peusner KD, Morest DK. The neuronal architecture and topography of the nucleus vestibularis tangentialis in the late chick embryo. Neuroscience. 1977a; 2:189–207. [PubMed: 904774]

Peusner KD, Morest DK. A morphological study of neurogenesis in the nucleus vestibularis tangentialis of the chick embryo. Neuroscience. 1977b; 2:209–227. [PubMed: 904775]

Peusner KD, Giaume C. Ontogeny of electrophysiological properties and dendritic pattern in second-order chick vestibular neurons. J Comp Neurol. 1997; 384:621–633. [PubMed: 9259493]

Popratiloff A, Peusner KD. Otolith fibers and terminals in chick vestibular nuclei. J Comp Neurol. 2007; 502:19–37. [PubMed: 17335047]

Puelles, L.; Martinez-de-la-Torre, M.; Paxinos, G.; Watson, C.; Martinez, S. The Chick Brain In Stereotaxis Coordinates. Academic Press; 2007.

Ramon y Cajal S. Les ganglions terminaux du nerf acousticque des oiseaux. Trab Lab Invest Biol Univ Madr. 1908; 6:195–224.

Rogers, LJ. The development of brain and behavior in the chicken. CAB International Press; Wallingford, UK: 1995.

Sanders EB. A consideration of certain bulbar, midbrain and cerebellar centers and fiber tracts in birds. J Comp Neurol. 1929; 49:155–222.

Saxon DW, Beitz AJ. The normal distribution and projections of constitutive NADPH-d/NOS neurons in the brainstem vestibular complex of the rat. J Comp Neurol. 2000; 425:97–120. [PubMed: 10940945]

NIH-PA Author Manuscript

NIH-PA Author Manuscript

NIH-PA Author Manuscript

Sekirnjak C, du Lac S. Physiological and anatomical properties of mouse medial vestibular nucleus neurons projecting to the oculomotor nucleus. J Neurophysiol. 2006; 95:3012–3023. [PubMed: 16436481]

Shao M, Hirsch JC, Giaume C, Peusner KD. Spontaneous synaptic activity is primarily GABAergic in vestibular nucleus neurons of the chick embryo. J Neurophysiol. 2003; 90:1182–1192. [PubMed: 12904504]

Shao M, Hirsch JC, Giaume C, Peusner KD. Spontaneous synaptic activity in chick vestibular nucleus neurons during the perinatal period. Neuroscience. 2004; 127:81–90. [PubMed: 15219671]

Shao M, Hirsch JC, Peusner KD. Maturation of firing pattern in chick vestibular nucleus neurons. Neuroscience. 2006a; 141:711–726. [PubMed: 16690214]

Shao M, Hirsch JC, Peusner KD. Emergence of action potential generation and synaptic transmission in vestibular nucleus neurons. J Neurophysiol. 2006b; 96:1215–1226. [PubMed: 16775212]

Shao M, Gottesman-Davis A, Popratiloff A, Peusner KD. Dye coupling in developing vestibular nuclei. J Neurosci Res. 2008; 86:832–844. [PubMed: 17941057]

Shaw MD, Baker R. Direct projections from vestibular nuclei to facial nucleus in cats. J Neurophysiol. 1983; 50:1265–1280. [PubMed: 6319618]

Straka H, Vibert N, Vidal PP, Moore LE, Dutia MB. Intrinsic membrane properties of vertebrate vestibular neurons: Function, development and plasticity. Progress in Neurobiol. 2005; 76:349–392.

Tobias, PV. The upright head in hominid evolution.. In: Berthoz, A.; Vidal, PP.; Graf, W., editors. The Head-Neck Sensory Motor System. Oxford University Press; New York: 1992.

Wahl CM, Noden DM, Baker R. Developmental relations between sixth nerve motor neurons and their targets in the chick embryo. Dev Dyn. 1994; 201:191–202. [PubMed: 7873790]

Whiteside TCD. The head movement of walking birds. J Physiol (Lond). 1967; 188:31P.

Wild JM. Vestibular projections to the thalamus of the pigeon: an anatomical study. J Comp Neurol. 1988; 271:451–60. [PubMed: 2454968]

Wold JE. The vestibular nuclei in the domestic hen (*Gallus domesticus*): Ascending projections to the mesencephalic eye motor nuclei. J Comp Neurol. 1978; 179:393–406. [PubMed: 641224]

Yamanaka T, Him A, Cameron SA, Dutia MB. Rapid compensatory changes in GABA receptor efficacy in rat vestibular neurones after unilateral labyrinthectomy. J Physiol. 2000; 523:413–424. [PubMed: 10699085]

Zhao M, Wu SH. Morphology and physiology of neurons in the ventral nucleus of the lateral lemniscus in rat brain slices. J Comp Neurol. 2001; 433:255–271. [PubMed: 11283963]

NIH-PA Author Manuscript

NIH-PA Author Manuscript

NIH-PA Author Manuscript

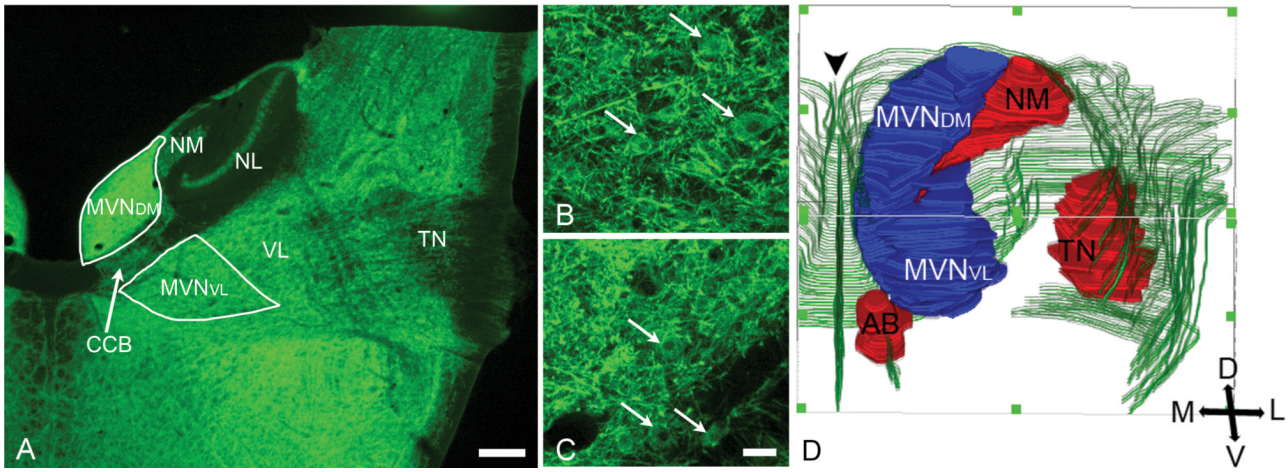

Fig. 1.

A, MAP2-labeled transverse section (50 μm) (4x objective) of H5 chicken brainstem at the level of entry of the primary vestibular fibers into the medulla oblongata. TN, tangential nucleus (central level); VL, ventrolateral vestibular nucleus; MVN_{DM}, dorsomedial part of MVN; MVN_{VL}, ventrolateral part of MVN; NL, nucleus laminaris; NM, nucleus magnocellularis; CCB, crossed cochlear bundle. **B**, **C**, 20x images of MVN_{DM} and MVN_{VL}, respectively, showing the cytology of MAP2-labeled MVN neurons (arrows). In **A-C**, dorsal is to the top and medial is to the left. **D**, Three dimensional reconstruction from sections like **A** depicting the MVN (blue); TN, NM, AB (abducens nucleus) (red); surface of the brainstem and cranial nerves (green). The midline is indicated by arrowhead. Posterior is to the top, anterior is to the bottom.

NIH-PA Author Manuscript
NIH-PA Author Manuscript
NIH-PA Author Manuscript

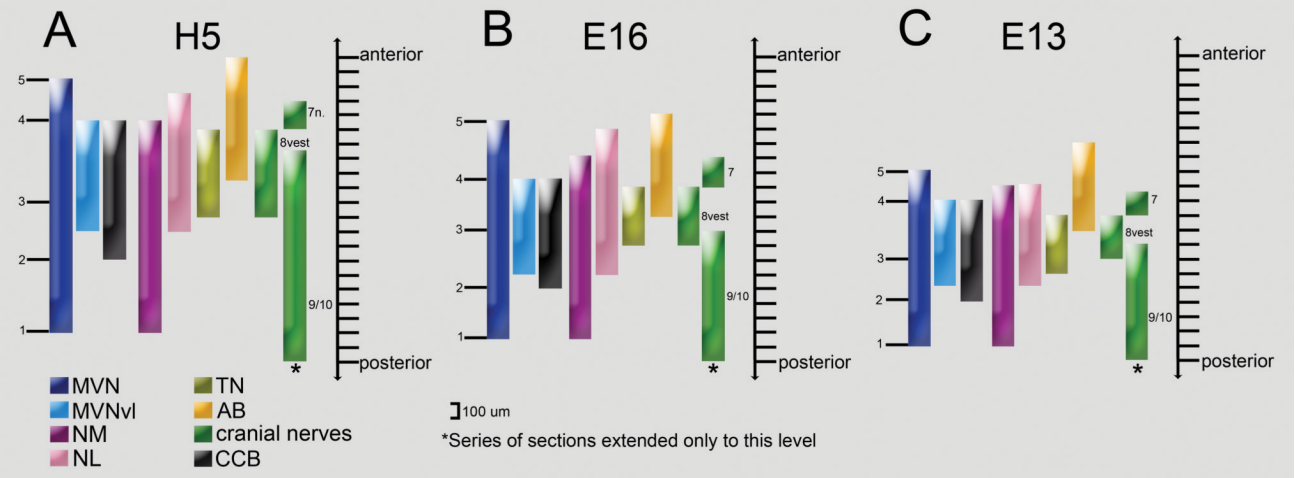

Fig. 2.

Diagrams depicting the anteroposterior extent of the chicken MVN in relation to other nuclei, cranial nerves, and the crossed cochlear bundle (CCB). MVN is subdivided into five sequential levels from posterior (1) to anterior (5): (1) posterior tip of MVN, (2) level at which the CCB first appears, (3) MVN mid-point at the level of tangential nucleus (TN), (4) level at which the CCB disappears, and (5) anterior tip of MVN. MVN, medial vestibular nucleus; $MVN_{VL,}$ ventrolateral part of MVN; NM, nucleus magnocellularis; NL, nucleus laminaris; AB, abducens nucleus; 8vest, vestibular nerve.

NIH-PA Author Manuscript

NIH-PA Author Manuscript

NIH-PA Author Manuscript

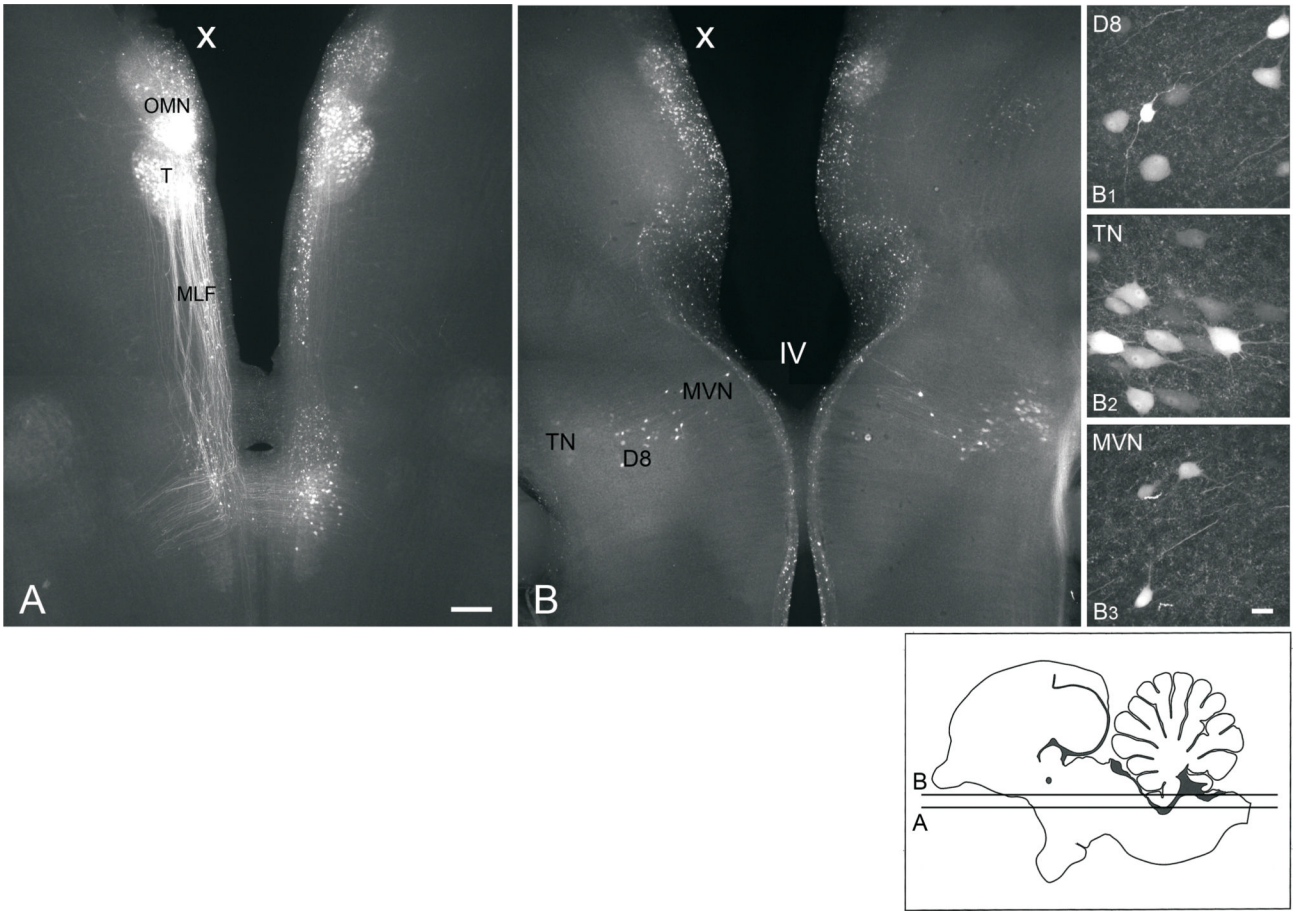

Fig. 3.

A, **B**, Low power, conventional fluorescence images (4x objective) of 300 μm, horizontal sections prepared from an E13 brainstem preparation, which received a unilateral extracellular biocytin injection into the oculomotor nucleus (X, injected side). Section **B** is dorsal to section **A**. **B_1-B_3**, high-power confocal images (40x objective) of retrogradely labeled neurons in the ipsilateral descending vestibular nucleus (D8), contralateral tangential nucleus (TN), and ipsilateral MVN, respectively, which appear in low power in **B**. The focal plane for **B_1-B_3** may differ from each other and **B**. Insert, diagram of sagittal section of the brainstem indicating the levels of **A** and **B**. Scale bar in **A**, 200 μm, also refers to **B**. Scale bar in **B_3**, 25 μm, also refers to **B_1** and **B_2**. All photomicrographs are oriented with anterior to the top.

NIH-PA Author Manuscript
NIH-PA Author Manuscript
NIH-PA Author Manuscript

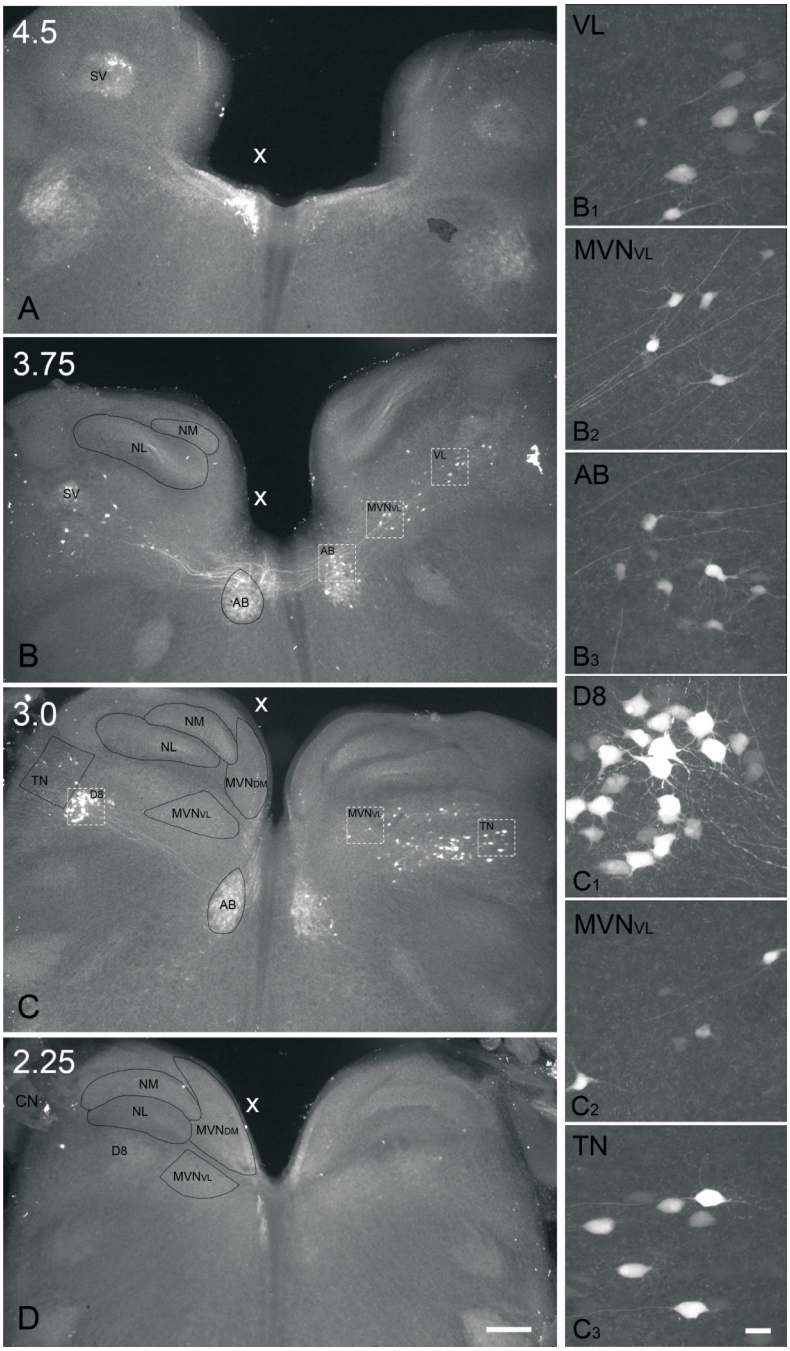

Fig. 4.

Low power, conventional fluorescence images (4x objective) of 300 μm thick transverse sections in series prepared from an E13 brainstem preparation which received a unilateral extracellular biocytin injection into the oculomotor nucleus. The injected side is indicated (X). Sections are arranged from anterior (**A**) to more posterior levels (**D**). **A**, level 4.5, anterior tip of MVN; **B**, level 3.75, central abducens nucleus (AB); **C**, level 3.0, central tangential nucleus (TN); **D**, level 2.25, cochlear nerve (CN) entry into brainstem. Scale bar, 200 μm. **B_1-C_3**, high power confocal images (40x objective) of neurons from sections **B** and **C,** respectively**. B_1,** ventrolateral vestibular nucleus (VL) neurons contralateral to the

NIH-PA Author Manuscript

NIH-PA Author Manuscript

NIH-PA Author Manuscript

injection site; **B_2,** MVN_{VL} neurons contralateral to the injection site; **B_3,** abducens nucleus (AB) neurons contralateral to the injection site. **C_1,** descending vestibular nucleus (D8) neurons ipsilateral to the injection site; **C_2,** MVN_{VL} neurons contralateral to the injection site; **C_3,** tangential nucleus (TN) neurons contralateral to the injection site. Scale bar in **D**, 200 μm, refers to **AD**. Scale bar in **C_3**, 25 μm, refers to **B_1-C_3**. In all photomicrographs, dorsal is to the top.

NIH-PA Author Manuscript
NIH-PA Author Manuscript
NIH-PA Author Manuscript

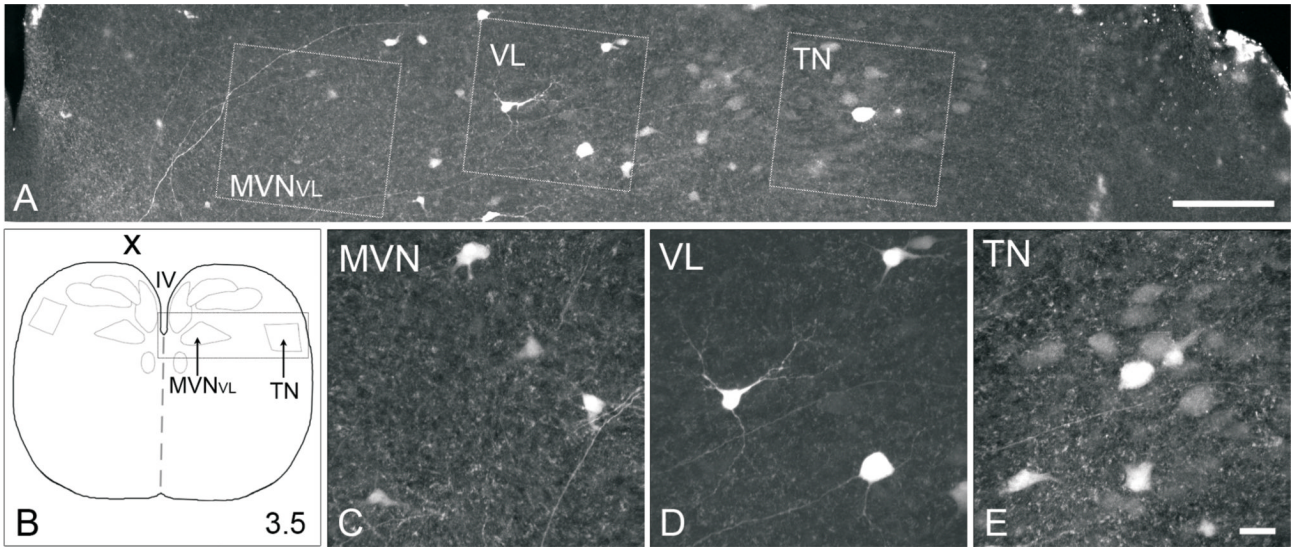

Fig. 5.

A, Confocal image (20x objective) of 300 μm, transverse section from E13 brainstem preparation, which received a unilateral biocytin injection into the contralateral trochlear nucleus. **B,** diagram of transverse section of brainstem, with a box indicating the region from which section **A** is taken. **C-E,** High-power confocal images (40x objective) of retrogradely labeled neurons from MVN_{VL}, ventrolateral vestibular nucleus (VL), and tangential nucleus (TN), which were boxed in **A**. The focal plane for **C-E** may differ from each other and **A**. In all photomicrographs, dorsal is to the top, and medial is to the left. Scale bar in **A**, 250 μm; scale bar in **E**, 25 μm, refers to **C-E**.

NIH-PA Author Manuscript
NIH-PA Author Manuscript
NIH-PA Author Manuscript

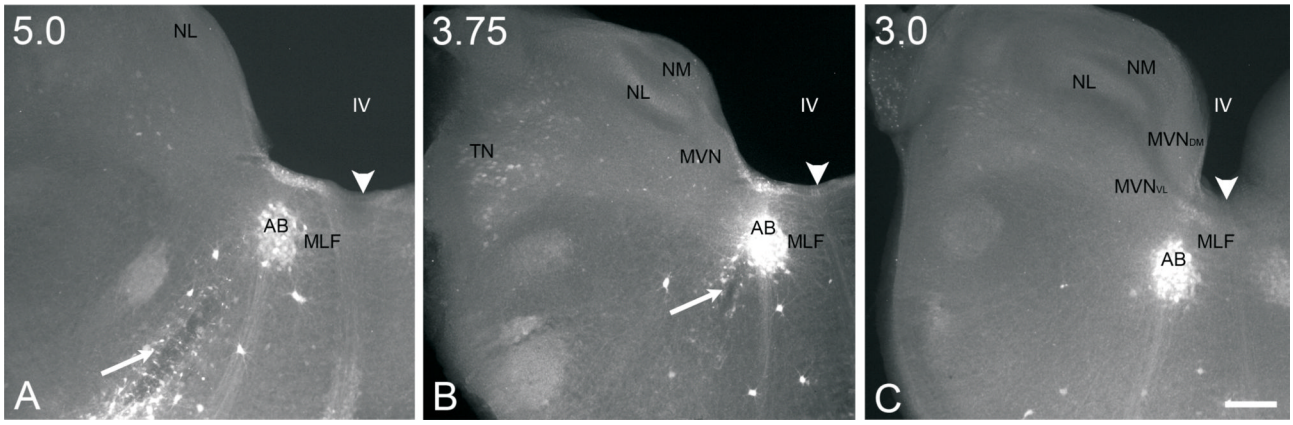

Fig. 6.

Low power conventional fluorescence images (4x) of 300 μm, transverse serial sections of E13 brainstem preparation that received a biocytin injection into the abducens nucleus (AB). Sections are arranged from anterior (**A**) to posterior levels (**C**). The level of each section is indicated in the upper left corner. NL, nucleus laminaris; NM, nucleus magnocellularis; TN, tangential nucleus; MVN_{VL}, ventrolateral part of MVN; MVN_{DM}, dorsomedial part of MVN. IV, fourth ventricle. **A**, **B**, Arrows indicate the path of the injection pipet; arrowhead, midline. Scale bar, 200 μm.

NIH-PA Author Manuscript

NIH-PA Author Manuscript

NIH-PA Author Manuscript

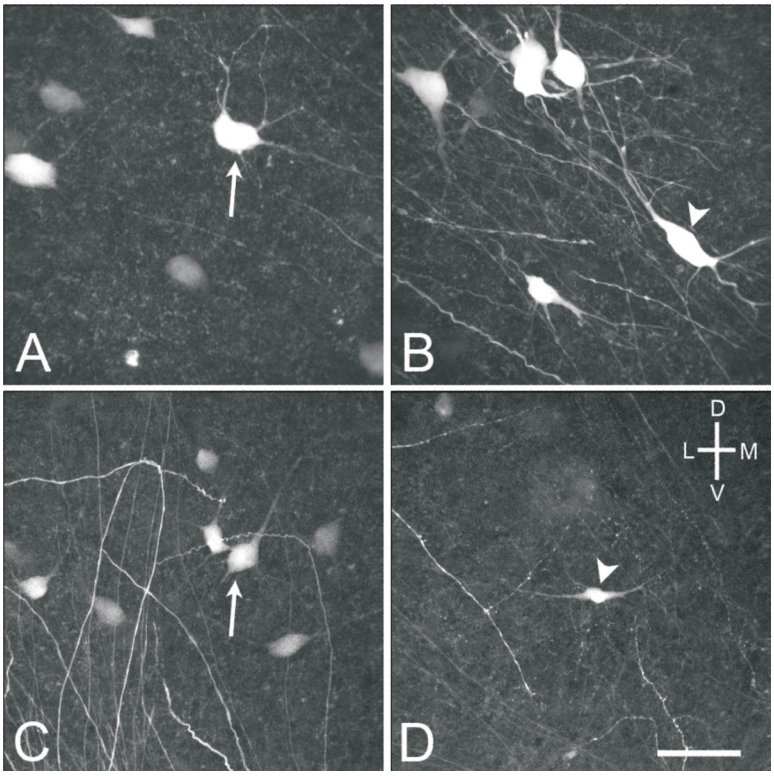

Fig. 7.

High power (40x objective) confocal images of MVN_{VL} stellate (arrows) and elongate (arrowheads) neurons from E16 brainstem preparations. **A**, Stellate cell labeled after injecting the contralateral oculomotor nucleus. **B**, Elongate cell labeled after injecting the contralateral oculomotor nucleus. **C**, Stellate cell labeled after injection the contralateral abducens nucleus. **D**, Elongate cell labeled after injecting the ipsilateral abducens nucleus. Scale bar, 50 μm.

NIH-PA Author Manuscript
NIH-PA Author Manuscript
NIH-PA Author Manuscript

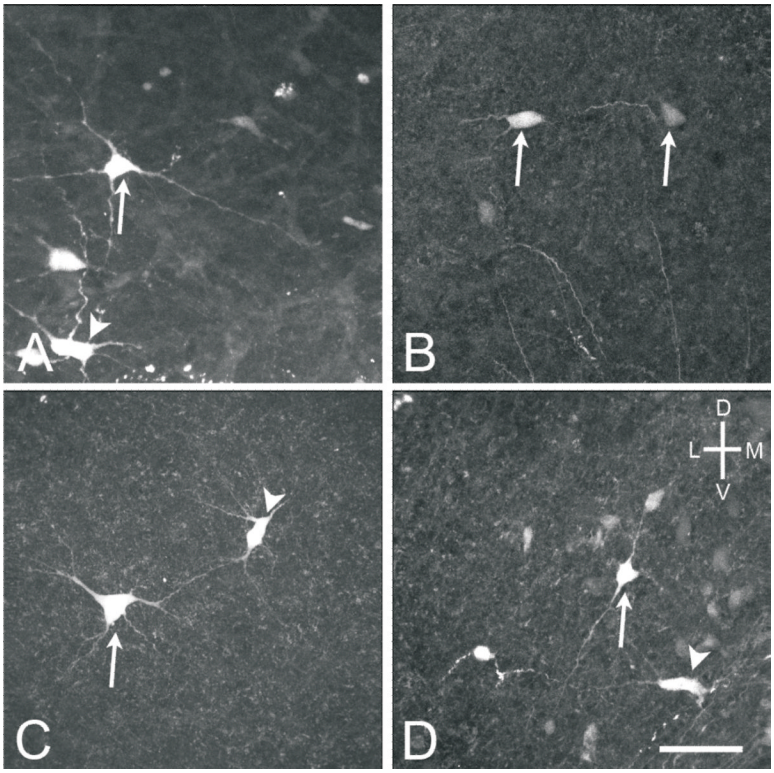

Fig. 8.

High power (40x objective) confocal images of MVN_{VL} stellate (arrows) and elongate (arrowheads) neurons labeled after abducens nucleus injections. **A**, E13, stellate and elongate cells ipsilateral to the injected nucleus from a brainstem preparation. **B**, E13, two stellate neurons contralateral to the injected nucleus from a brain slice preparation. **C**, E16, stellate and elongate cells ipsilateral to the injected nucleus from a brainstem preparation. **D**, E16, stellate and elongate cells contralateral to the injected nucleus from a brain slice preparation. Scale bar, 50 μm.

NIH-PA Author Manuscript
NIH-PA Author Manuscript
NIH-PA Author Manuscript

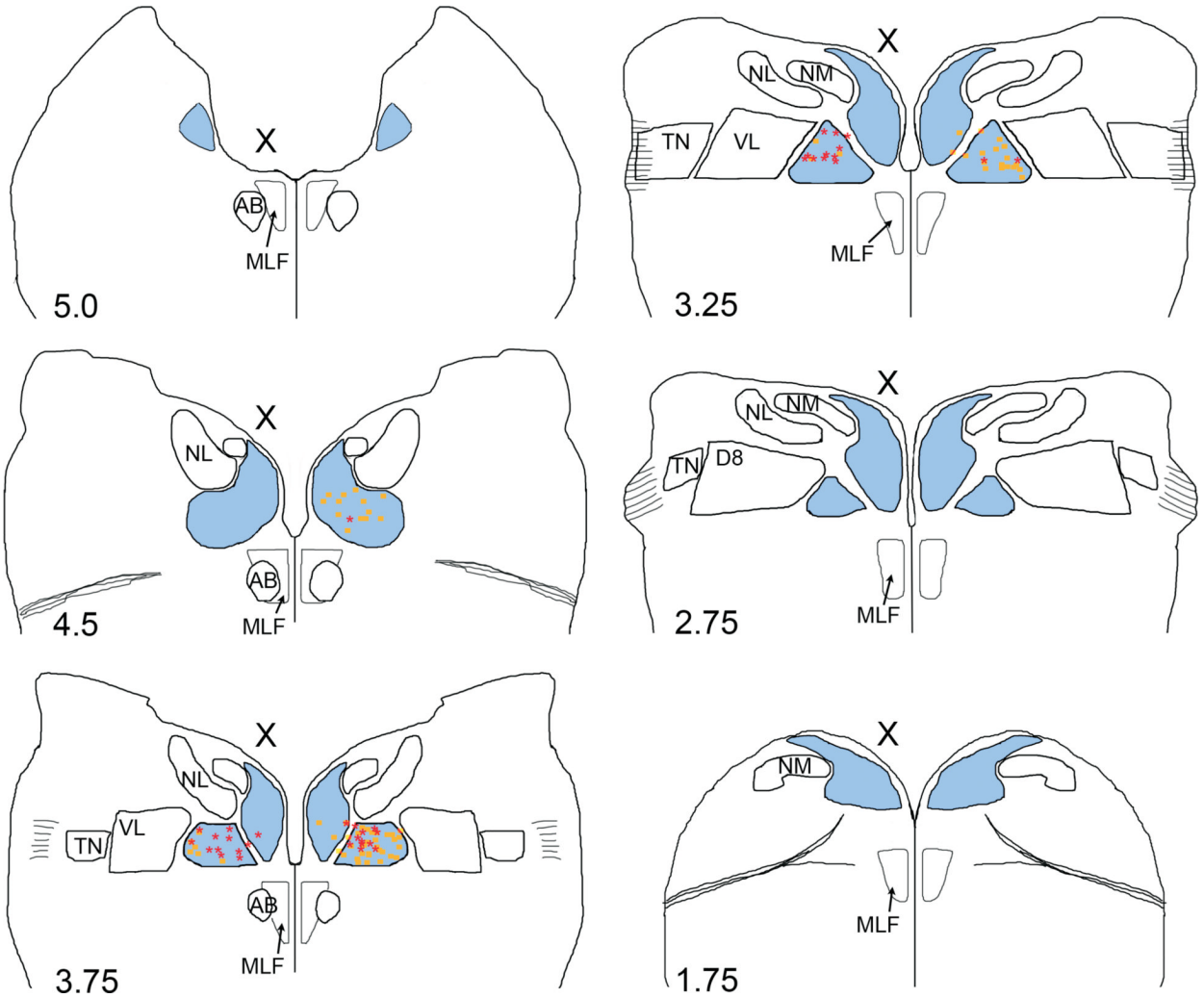

Fig. 9.

Summary diagram of brainstem sections showing the locations of retrogradely labeled MVN neurons after brainstem injections into the oculomotor (yellow squares, n=3 animals) or abducens nucleus (red stars, n=3 animals) at E13. The anteroposterior levels of the brainstem sections are labeled with reference to Fig. 2. Outlines are arranged from anterior (top left) to posterior (bottom right). To correct for tilt in the section plane, the level of each side of the section was evaluated independently to determine the anteroposterior level. The injected side is indicated (X). MVN (blue); NM, nucleus magnocellularis; NL, nucleus laminaris, TN, tangential nucleus; D8, descending vestibular nucleus; VL, ventrolateral vestibular nucleus, MLF, medial longitudinal fasciculus.

NIH-PA Author Manuscript

NIH-PA Author Manuscript

NIH-PA Author Manuscript

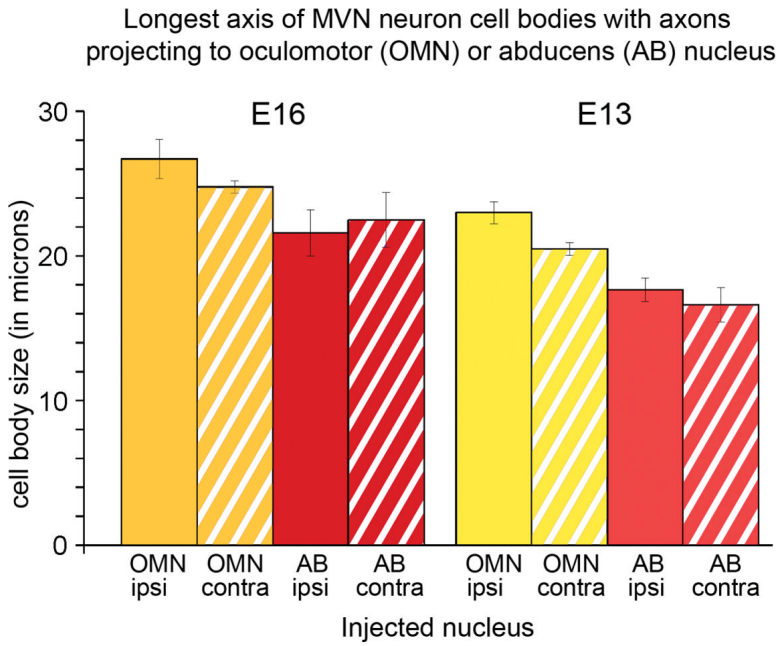

Fig. 10.

Histogram showing the mean values for the longest cell body axis of MVN neurons retrogradely labeled after biocytin was injected into either the oculomotor (OMN) or abducens nucleus (AB) on one side. Neurons are grouped according to the nucleus which they project to and whether the projection terminated in the ipsi- or contralateral nucleus. E16, OMN ipsi, n=10; E16, OMN contra, n=79; E16, AB ipsi, n=5; E16, AB contra, n=4; E13, OMN ipsi, n=10; E13, OMN contra, n=62; E13, AB ipsi, n=23; E13, AB contra, n=13.

NIH-PA Author Manuscript
NIH-PA Author Manuscript
NIH-PA Author Manuscript

Table I

Number of retrogradely labeled neurons in vestibular nuclei after unilateral biocytin injections in brainstem preparations (transverse sections)

		Ipsilateral						Contralateral					
Animal	**Injection site**	**MVN_{DM}**	**MVN_{VL}**	**TN**	**D8**	**VL**	**SV**	**MVN_{DM}**	**MVN_{VL}**	**TN**	**D8**	**VL**	**SV**
WL2041007	OMN, E13	**0**	**0**	45	0	5	0	**0**	**1**	45	0	5	0
WL2091107	OMN, E13	**0**	**3**	0	45	0	15	**7**	**16**	17	50	0	5
WL2091207	OMN, E13	**0**	**4**	0	30	15	20	**6**	**26**	15	35	15	0
WL3041007	OMN, E13	**0**	**1**	25	20	15	9	**1**	**8**	20	45	10	0
WL1041607	OMN, E16	**0**	**4**	15	45	40	15	**1**	**22**	20	60	60	10
WL1091707	OMN, E16	**0**	**0**	0	30	10	20	**4**	**14**	15	65	20	0
WL1091807	OMN, E16	**0**	**2**	35	20	30	17	**0**	**15**	50	20	50	0
WL2041607	OMN, E16	**0**	**1**	50	20	11	15	**0**	**9**	50	35	10	7
WL2091907	OMN, E16	**0**	**4**	45	25	35	5	**0**	**17**	20	35	50	0
WL1110807	TRO, E13	**0**	**0**	0	0	2	5	**0**	**13**	12	10	25	5
WL1110907	TRO, E16	**0**	**0**	35	0	15	2	**1**	**12**	15	5	2	2
WL1060408	AB, E13	**1**	**7**	28	5	5	0	**0**	**6**	0	8	3	0
WL2051908	AB, E13	**0**	**9**	2	6	6	4	**0**	**1**	15	2	9	4
WL3052008	AB, E13	**0**	**8**	15	10	5	3	**0**	**5**	0	3	7	5
WL3060908	AB, E16	**1**	**8**	95	45	45	0	**0**	**4**	90	40	25	0

J Neurosci Res. Author manuscript; available in PMC 2013 March 22.

NIH-PA Author Manuscript
NIH-PA Author Manuscript
NIH-PA Author Manuscript

Table II

MVN neuron morphology after biocytin injections in brainstem preparations

	Oculomotor injection (n=9 preparations at E13 and E16)				Abducens injection (n=4 preparations at E13 and E16)			
	Stellate		Elongate		Stellate		Elongate	
Level of MVN	Ipsilateral	Contralateral	Ipsilateral	Contralateral	Ipsilateral	Contralateral	Ipsilateral	Contralateral
1-2	0	0	0	0	0	0	0	0
2-3	0	16	0	0	10	2	1	1
3-4	14	87	0	6	20	12	1	3
4-5	6	40	0	2	0	2	1	0